Phase transitions inK2ZnCl4

Phase transitions in K₂ZnCl₄

H. M. Lu and J. R. Hardy
Department of Physics and Center for Electro-Optics, University of Nebraska–Lincoln, Lincoln, Nebraska 68588-0111

Abstract

It is shown that the potential-energy surface in K_2ZnCl_4 contains a double-well structure, very similar to some of the other A_2BX_4 compounds (e.g., K_2SeO_4, Rb_2ZnCl_4), except that the double well is much deeper and broader, giving rise to a highly disordered high-temperature phase as observed experimentally. A lattice-dynamics study of the $Pna2_1$ structure shows an instability with the wave vector $q=0.5b^*+(0.5\pm\delta)c^*$, providing an explanation to the incommensurate phase transition reported recently.

Brief Reports

Phase transitions in K_2ZnCl_4

H. M. Lu and J. R. Hardy

Department of Physics and Center for Electro-Optics, University of Nebraska–Lincoln,
Lincoln, Nebraska 68588-0111

It is shown that the potential-energy surface in K_2ZnCl_4 contains a double-well structure, very similar to some of the other A_2BX_4 compounds (e.g., K_2SeO_4, Rb_2ZnCl_4), except that the double well is much deeper and broader, giving rise to a highly disordered high-temperature phase as observed experimentally. A lattice-dynamics study of the $Pna2_1$ structure shows an instability with the wave vector $q=0.5b^*+(0.5\pm\delta)c^*$, providing an explanation to the incommensurate phase transition reported recently.

For a long time, K_2ZnCl_4 has been considered to have the same phase sequence as Rb_2ZnCl_4.[1] It has the β-K_2SO_4 structure ($Pnam$) at high temperatures, like many other members in the family of the A_2BX_4 compounds. At 553 K (T_i), it transforms to an incommensurate phase with the incommensurate modulation vector $q=[(1-\delta)a^*]/3$, where a^* is the first reciprocal-lattice vector along the [100] direction and $\delta \ll 1$. At 403 K (T_{c1}) the incommensurate modulation disappears and the system locks into a ferroelectric superstructure ($Pna2_1$) whose a axis is triple that of the $Pnam$ phase. When cooled further, it undergoes another transition at 145 K (T_{c2}) to a monoclinic structure ($C1c1$). However, it was found recently that K_2ZnCl_4 has another incommensurate phase just above the lower-temperature monoclinic phase, while Rb_2ZnCl_4 has not.[2,3] Reference 3 gave the temperature range for this phase as 140–144 K and revealed, by inelastic neutron scattering, a soft optic phonon with the wave vector $q=(0.5b^*+(0.5\pm\delta)c^*$ responsible for the incommensurate phase transition.

In the present paper, we perform structural relaxation, molecular-dynamics simulation, and lattice-dynamics calculations of K_2ZnCl_4 using a recent first-principles approach to ionic molecular crystals.[4,5] The method starts from *ab initio* quantum chemistry calculations regarding the whole molecular ions, i.e., the $ZnCl_4^{2-}$ ions in the present case, as single entities and then uses the resultant realistic electron charge density to calculate the Gordon-Kim pair potentials,[6] thereby correctly treating the effects of intramolecular covalency on the intermolecular interactions. For the intramolecular interactions, which are beyond the Gordon-Kim model and the pairwise interaction scheme, a harmonic expansion is employed, with the expansion coefficients also determined by *ab initio* quantum chemistry calculations. In our previous study of Rb_2ZnCl_4,[5] we have performed the quantum

chemistry calculations for the free molecular ion $ZnCl_4^{2-}$ and therefore we can simply take those results, since the $ZnCl_4^{2-}$ ions take essentially the same form of modestly distorted tetrahedra in both Rb_2ZnCl_4 and K_2ZnCl_4.[7,8] Thus, we will use the same intramolecular harmonic expansions and we will use the same electron charge densities for the Zn and Cl atoms to compute the Gordon-Kim pair potentials,[6] together with the charge density for the K^+ ion.[9] Considering the good and fairly broad agreement between theory and experiment in the study[5] of Rb_2ZnCl_4, it is expected that these pair potentials and the intramolecular harmonic expansion will give a reasonable description for the potential energy of the present system.

In order to test the quality of our interionic potentials, we first performed a static energy minimization for the $Pna2_1$ structure of K_2ZnCl_4. Our relaxation started from the experimental structure[10] and was subject to the constraints of the $Pna2_1$ symmetry. The minimization was for an infinite lattice, obtained by applying periodic boundary conditions, and the standard technique of Ewald summation was used for the calculations of lattice energies and forces, etc. Figure 1 shows the bc cross sections of the experimental (a) and theoretical (b) $Pna2_1$ structures. The bonds between a Zn atom and its four nearest neighbors are shown by straight lines. As can be seen, each of the $ZnCl_4^{2-}$ molecular ions has a Zn—Cl bond that is close to being parallel to the b axis. In the high-temperature $Pnam$ structure above the $Pna2_1$ phase, these bonds should be *exactly* parallel to the b axis in projections like Fig. 1 and the three $ZnCl_4^{2-}$ ions that sit along the a axis have identical orientations. Therefore, the tripled $Pna2_1$ structure can be seen to be a result of a modulation that mainly rotates the $ZnCl_4^{2-}$ ions about the a axis and correspondingly shifts the K^+ ions in the c direction. Clearly, the theoretical structure well reproduced this modulation, only the modulation amplitude is

about 20% too large. This should not be surprising, since the experimental data are obtained at $T=300$ K, while the static relaxed theoretical structure corresponds to $T=0$ K. In fact, we have performed a molecular-dynamics simulation at 300 K and found that the modulation amplitude in the average structure is approximately 70% of that in the static relaxed structure in Fig. 1(b), which is then much closer to that in the experimental structure.

The lattice constants in the relaxed structure are $a=49.143$, $b=22.205$, and $c=13.447$ a.u., all shorter than the experimental values (2.9% for a, 5.3% for b, and 1.9% for c). This has been a rather general feature for large unit-cell simulations using Gordon-Kim potentials and it appeared similarly in our studies[4,5] of K_2SeO_4 and Rb_2ZnCl_4. Although these deviations are certainly large in magnitude, they are, however, percentagewise comparable in all three dimensions. The reduced basis parameters in the relaxed structure[11] are in close agreement with the experimental values. The coordinations of the Zn and K atoms are reproduced satisfactorily. While larger differences appear between the theoretical and experimental values for some Cl atoms, they are due to the larger modulation in the theoretical structure as discussed above. Overall, the theoretical structure is more or less uniformly contracted and should still preserve the basic symmetries of the system relevant to the phase transitions under study.

In our previous studies of K_2SeO_4 (Ref. 4) and Rb_2ZnCl_4,[5] it was found that the potential-energy surface
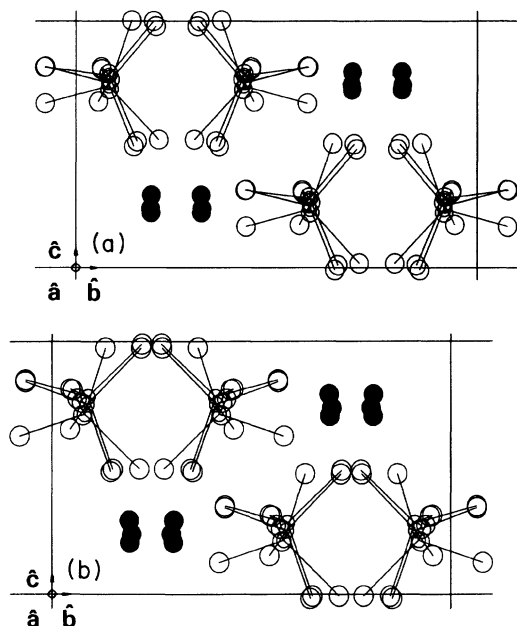

FIG. 1. Projections along the a axis of the (a) experimental and (b) theoretical $Pna2_1$ structures of K_2ZnCl_4. Unit vectors indicate the directions of the lattice axes. A unit vector pointing out of the page is represented by a circle. The Zn and Cl atoms are represented by small and large open circles, respectively. Bonds (straight lines) connect each Zn and the four nearest Cl atoms. The K atoms are represented by solid circles, except those obscured by the other atoms.

pertinent to the phase transitions, i.e., the incommensurate and the subsequent triple lock-in transitions, contains a double well when described using a single $Pnam$ unit cell. On top of the double well is the high-temperature $Pnam$ structure, while at the bottom are two stable monoclinic structures (the angle between the b and c axes $\alpha \neq 90°$) that have exactly the same potential energy but look like mirror images to each other. These monoclinic structures are the results of a lock-in of the zone-center instability in the $Pnam$ structure. Since K_2ZnCl_4 also has the same incommensurate and triple lock-in transitions as K_2SeO_4 and Rb_2ZnCl_4, we expect to find the same double-well structure on the potential surface. Thus, we performed a static relaxation for the $Pnam$ structure of K_2ZnCl_4 and then computed dispersion curves for the relaxed structure. We found, indeed, a zone-center instability just like that in the other two compounds, which leads to exactly the same kind of monoclinic structures as those in K_2SeO_4 and Rb_2ZnCl_4. Therefore, the potential-energy surface for a single $Pnam$ cell of K_2ZnCl_4 indeed has a double-well structure. When multiple cells are involved, this generates a multiple-well structure on the total potential-energy surface which provides the basis for the incommensurate and the cell-tripling phase transitions observed in these systems.

However, the double well in K_2ZnCl_4 is deeper than that in Rb_2ZnCl_4 and much deeper than that in K_2SeO_4. If measured by the difference between the static potential energies of the $Pnam$ structure and of the two energetically equivalent monoclinic structures, the depths for K_2SeO_4, Rb_2ZnCl_4, and K_2ZnCl_4 are 12.3, 109.8, and 207.3 meV per formula unit, respectively. Moreover, the angles α in the monoclinic structures of K_2SeO_4, Rb_2ZnCl_4, and K_2ZnCl_4 are 88°, 84°, and 82°, respectively, indicating that the double well in K_2ZnCl_4 is broader than that in Rb_2ZnCl_4, and much broader than that in K_2SeO_4. Therefore, from K_2SeO_4 to Rb_2ZnCl_4, and then to K_2ZnCl_4, the double well gets deeper and broader. This agrees with the sequence of the $Pnam$ incommensurate transition temperatures in these compounds,[1] 129.5 K in K_2SeO_4, 303 K, in Rb_2ZnCl_4, and 553 K in K_2ZnCl_4. It is also consistent with the experimental observation[12-14] that the $Pnam$ phases of both Rb_2ZnCl_4 and K_2ZnCl_4 are much more disordered than that of K_2SeO_4.

The static energy for the relaxed $Pna2_1$ structure is 163 meV per formula units lower than that for the $Pnam$ structure, but 45 meV higher than that for the singlet monoclinic structures found above. However, in experiment the system transforms from the $Pnam$ phase to the tripled $Pna2_1$ structure rather than to the singlet structure with a lower static energy. This is very similar to the situations in K_2SeO_4 (Ref. 4) and Rb_2ZnCl_4,[5] and can be explained with a similar argument. When the temperature is above 550 K and the system is in the $Pnam$ phase, the relatively small difference in energy between the tripled and the singlet structures makes the two effectively degenerate. Consequently, as the temperature decreases, the $Pnam$ structure begins to transform and

the state selected will be that of higher *entropy*. Clearly, this is the $Pna2_1$ phase in which the molecular ions have three, rather than one, possible orientations. Subsequently, for the $Pna2_1$ structure to transform to the singlet monoclinic structure, it requires that at least one of the tetrahedra switch through the $Pnam$ configuration and, as the system is cooled further, this becomes increasingly difficult. When the temperature is lowered further so that the singlet monoclinic structure becomes preferred energetically, the transformation is frustrated by the ~ 160-meV barrier and the $Pna2_1$ phase persists.

A lattice-dynamics study[5] of the static relaxed theoretical $Pna2_1$ structure of Rb_2ZnCl_4 has shown that an instability exists at the point $q=(b^*+c^*)/2$, predicting a soft phonon transition that will double the unit cell along both the b and c axes, just as observed in experiment.[3] We thus calculated the dispersion curves along the [011] direction for the static relaxed theoretical $Pna2_1$ structure given [Fig. 1(b)], and plotted them in Fig. 2. The lowest four branches have the same shape as those in Rb_2ZnCl_4, but they have positive values at the zone boundary, rather than negative values, indicating that the structure in Fig. 1(b) would not be able to produce a similar lower-temperature structure as in Rb_2ZnCl_4, contrary to the experimental fact.

This discrepancy is, however, artificial, if we recall that the theoretical structure in Fig. 1(b) has a much larger cell-tripling modulation amplitude than the experimental structure in Fig. 1(a), due to the fact the former is for $T=0$ K, while the latter is for $T=300$ K. When we calculate the dispersion curves along the [011] direction for the theoretical static $Pnam$ structure of K_2ZnCl_4, we found that the boundary point $q=(b^*+c^*)/2$ is, in fact, *unstable*, which is found also to be true for Rb_2ZnCl_4. Therefore, it is the artificially large modulation from the $Pnam$ structure to the $Pna2_1$ structure in Fig. 1(b) that diminishes the $q=(b^*+c^*)/2$ instability in K_2ZnCl_4.

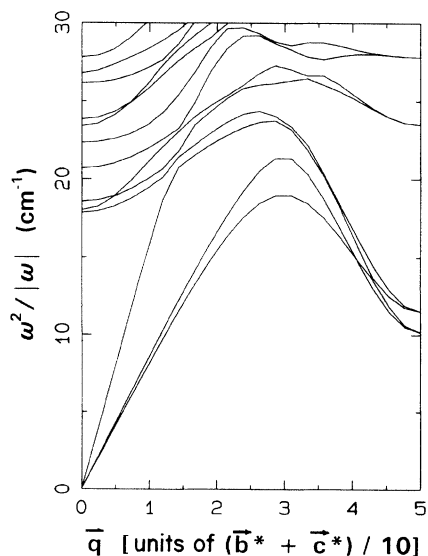However, in experiment, it is the instability in the structure at 300 K, not at 0 K, that determines the phase diagram.

In order to illustrate this point better, we computed dispersion curves for structures obtained by "stepping" from the theoretical $Pnam$ structure to the theoretical $Pna2_1$ structure linearly. In Fig. 3, we plot the lowest branch of the dispersion curves from the X point $q=b^*/2$ to the T point $q=(b^*+c^*)/2$ for each of the $Pnam$, $Pna2_1$, and three intermediate structures I, II, and III representing 25, 50, and 75 % of the total modulation in Fig. 1(b), respectively. We also performed similar calculations for Rb_2ZnCl_4 and plot the results in Fig. 4, since experimentally the two compounds behave differently—K_2ZnCl_4 has an extra incommensurate phase transition at 144 K above the cell-doubling transition at 140 K.[3]

In Fig. 3, we see that, even at the intermediate structure III, corresponding to a temperature of about $T=300$ K, the T point is still negative, indicating the instability for the cell-doubling transition. It is, indeed, the last extra 25% change in the structure that stabilizes the T point. The most interesting result is, however, that in Fig. 3 the minimum on the dispersion curve changes gradually from the X point to the T point, being at 0.42 for structure II and at 0.44 for structure III, while for Rb_2ZnCl_4 (Fig. 4) the change is sudden, i.e., no minimum occurred between the X and the T points for any of the dispersion curves. Since structures II and III better represent the actual crystal structure at finite temperatures, this shows that K_2ZnCl_4 should have a soft optic phonon-induced incommensurate phase transition with the wave vector $q=0.5b^*+(0.5\pm\delta)c^*$, which is consistent with the experimental observation.[3]
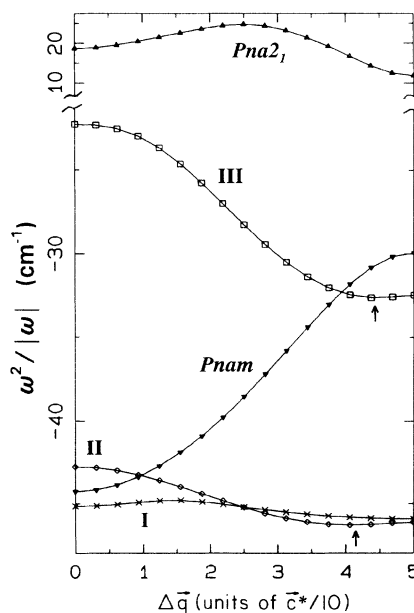
FIG. 3. The lowest dispersion curves from point $b^*/2$ to point $(b^*+c^*)/2$ for the $Pnam$ (∇), $Pna2_1$ ($\triangle$), and the intermediate structures I ($\times$), II ($\Diamond$), and III ($\square$) of K_2ZnCl_4. The arrows indicate the positions of the minimums on curves II and III.

FIG. 2. Dispersion curves along the [011] direction for the theoretical $Pna2_1$ structure of K_2ZnCl_4.
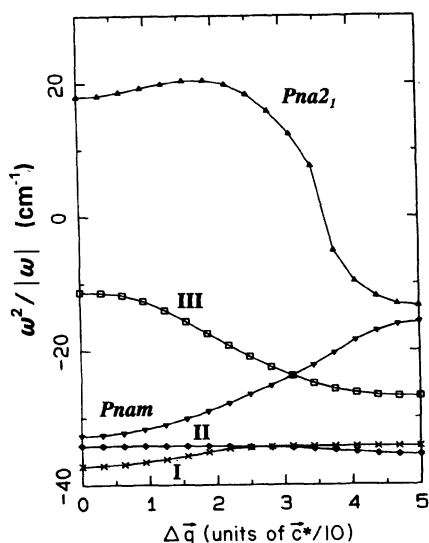
FIG. 4. Same as Fig. 3, except it is for Rb_2ZnCl_4.

Hoping to reproduce the lower temperature cell-doubling transition, we performed a molecular-dynamics "quench" for a supercell of 672 ions formed by doubling along b and quadrupling along c the $Pna2_1$ unit cell of K_2ZnCl_4. Our simulations followed a constant- (zero-) pressure algorithm and did not have any constraints besides the periodic boundary conditions necessary for simulating an infinite crystal. Starting from $T=300$ K, the sample was gradually cooled down by reducing the kinetic energy in steps. At each step, averages of atomic positions and lattice angles were taken over a period of 20 psec with the molecular-dynamics step size of 5 fsec. It was found that the angle between the a and c axes started to deviate from 90° around $T=250$ K, and increased to 90.7° at 20 K, while the other two lattice angles remained at 90° at all temperatures. Therefore, we have produced a monoclinic phase transition. But the average structure at the lower temperature was neither doubled in b nor in c, contrary to the experimental observation.[3]

We tend to believe that this discrepancy should be attributed to the limitations of the molecular-dynamics calculations, rather than to the quality of the ab initio interionic potentials; these potentials should be as good as those used in treating[5] Rb_2ZnCl_4 where close agreement with experiment was obtained for all the phase transitions, since the same description of the electron charge density of the $ZnCl_4^{2-}$ ion is used. One possible explanation could be that there are many metastable configurations that are very close in energy to the true ground state so that the molecular dynamics for a limited phase space and limited equilibration time is simply inadequate. In fact, this was the case for Rb_2ZnCl_4, where the similar molecular-dynamics "quench" resulted in a "wrong" ground-state structure with the monoclinic angle too large, although the structure was indeed doubled along both b and c directions.[5] Naturally, there may be other equally probable explanations as well. But, in any case, to clarify the situation requires simulations involving even longer equilibrium times and a still larger supercell, and is thus beyond the scope of the present report. Alternately, it may be that, since our supercell does not permit the new phase incommensurate along c to form, it also rules out formation of the commensurate T-point modulation if the former is an essential precondition for the latter to occur.

[1] H. Z. Cummins, Phys. Rep. **185**, 211 (1990), and references therein.

[2] K. Gesi, J. Phys. Soc. Jpn. **59**, 416 (1990).

[3] M. Quilichini, V. Dvorak, and P. Boutrouille, J. Phys. I France **1**, 1321 (1991).

[4] H. M. Lu and J. R. Hardy, Phys. Rev. Lett. **64**, 661 (1990); Phys. Rev. B **42**, 8339 (1990).

[5] H. M. Lu and J. R. Hardy, Phys. Rev. B **45**, 7609 (1992).

[6] R. G. Gordon and Y. S. Kim, J. Chem. Phys. **56**, 3122 (1972).

[7] M. Quilichini and J. Pannatier, Acta Crystallogr. B **39**, 657 (1983).

[8] M. Quilichini, G. Heger, and P. Schweiss, Ferroelectrics **79**, 117 (1988).

[9] E. Clementi and C. Roetti, At. Data Nucl. Data Tables **14**, 177 (1974).

[10] I. Mikhail and K. Peters, Acta Crystallogr. B **35**, 1200 (1979).

[11] Available on request.

[12] N. E. Massa, F. G. Ullman, and J. R. Hardy, Phys. Rev. B **27**, 1523 (1983).

[13] K. Itoh, A. Hinisada, H. Matsunaga, and E. Nakamura, J. Phys. Soc. Jpn. **52**, 664 (1983).

[14] V. Katkanant, J. R. Hardy, R. D. Kirby, and F. G. Ullman, Ferroelectrics **99**, 213 (1989).